Influence of system parameters on the hysteresis characteristics of a horizontal Rijke tube

Gopalakrishnan E. A.* and Sujith R. I.

Department of Aerospace Engineering, Indian Institute of Technology Madras
Chennai, 600036, India

(Submission date: September 25, 2013; Revised Submission date: February 13, 2014; Accepted date: May 9, 2014)

The influence of system parameters such as heater power, heater location and mass flow rate on the hysteresis characteristics of a horizontal Rijke tube is presented in this paper. It is observed that a hysteresis zone is present for all the mass flow rates considered in the present study. A power law relation is established between the non-dimensional hysteresis width and the Strouhal number, defined as the ratio between convective time scale and acoustic time scale. The transition to instability in a horizontal Rijke tube is found to be subcritical in all the experiments performed in this study. When heater location is chosen as the control parameter, period-2 oscillations are found for specific values of mass flow rate and heater power.

Keywords: Hysteresis; Subcritical Hopf bifurcation; Rijke tube; period-2 oscillations

1. INTRODUCTION

Thermoacoustic instability hampers the development of gas turbine engines, solid rocket motors, industrial burners and various other engineering systems where the prime source of energy is derived from combustion [1]. The instability occurs when the pressure fluctuations inherently present in a confinement are in phase with the heat release rate fluctuations of a heat source present in the same confinement [2]. The physical reasons of the origin of this instability need to be understood in order to implement effective control strategies. Systems which are susceptible to thermoacoustic instability are often too intricate to conduct a detailed investigation. This creates the need for a prototypical system which is simple enough to investigate, yet retains the essential dynamical features of the original system. A horizontal Rijke tube with a mesh type electrical heater is often chosen as a model system in literature [3–11].

In the case of a horizontal Rijke tube, it can be seen from earlier literature that beyond a critical value of the system parameter, there is a sudden change in qualitative behaviour of the system which takes the system from a stable state to an unstable state

*Corresponding author: gopalakrishnanea82@gmail.com

[4–11]. Sudden change in the qualitative behaviour of a system for an infinitesimal change in a system parameter is termed as a bifurcation in dynamical system literature [12]. If this change takes the system from a stable steady state to an oscillatory state it is termed as a Hopf bifurcation and the parameter value at which this change happens is called Hopf point [12, 13].

Hopf bifurcation can be classified into two categories (i) supercritical and (ii) subcritical based on the stability of the resulting oscillatory solutions (Fig. 1a & Fig. 1b). Supercritical bifurcation happens when the nonlinearity has a stabilizing influence and is characterized by the birth of low amplitude stable oscillatory solutions when the system becomes unstable. The asymptotic state (the state achieved by the system as time $t \to \infty$) of the system is independent of the initial conditions in the case of supercritical bifurcation. If the nonlinearity has a destabilizing influence on the system, then a subcritical bifurcation results. Small amplitude unstable oscillatory solutions are born when the control parameter reaches the point *B* (Fig. 1b) which is termed as Hopf point. The unstable oscillatory solutions will grow in amplitude as we move away from Hopf

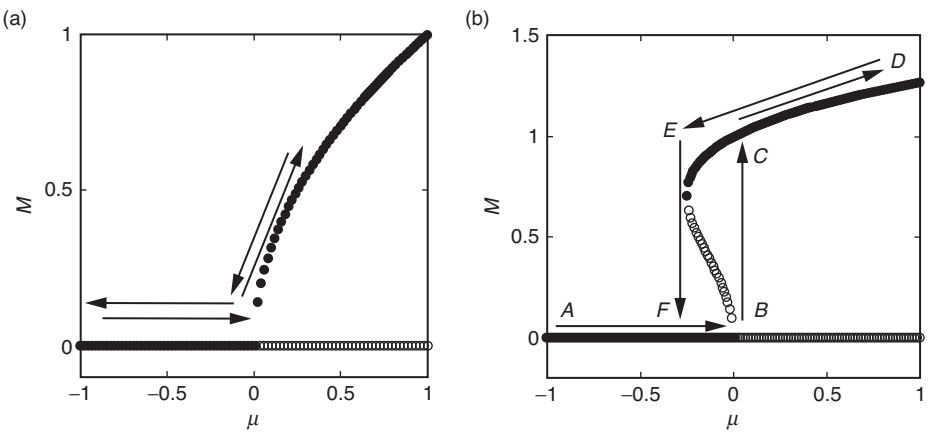

Figure 1: Bifurcation diagram depicting variation of a Measure *M* with a control parameter μ. (a) Supercritical bifurcation (b) Subcritical bifurcation. In supercritical bifurcation as the control parameter reaches the value of zero, low amplitude stable limit cycle oscillations are born. Unlike the supercritical bifurcation, large amplitude oscillatory solutions are present right at the onset of instability. The system is bistable in the hysteresis region *BCEF* and the stability of the system is dependent on the initial conditions in this region. • – Stable oscillatory solutions. ○ – Unstable oscillatory solutions. (The figures are obtained from the normal form equations of Hopf bifurcation.)

[1]It should be noted that the terminology '*stable oscillatory solution*' and '*unstable oscillatory solution*' refer to the stability of the oscillatory solutions and not that of the system. (i.e. the stability of the equilibrium state or fixed point.)

point[1]. As the system parameters reach some critical value; i.e.; when the control parameter is reduced till point *E*, unstable oscillatory solutions get stabilized through a fold bifurcation away from the Hopf point and the point *E* is called as the fold point [12–14] (Fig. 1b). Between the Hopf point and the fold point, the system has two stable asymptotic states, namely a stable oscillatory state and a stable steady state, hence the system is said to be bistable in this region and depending upon the initial conditions the system can either remain in the stable oscillatory state or in the stable steady state. Figure 1b shows that to bring the system back to a non-oscillatory state, the control parameter need to be reduced till the fold point '*E*'. The presence of a hysteresis zone (Region '*BCEF*' in Fig. 1b) is an important characteristic of subcritical transitions, where the system can remain in more than one state. It is to be noted that the system is said to be stable if it is in a steady state and it is said to be unstable if it is in an oscillatory state.

In short, if the transition is subcritical, the stability of the system in the hysteresis zone is dependent on initial conditions such that the system is stable to perturbations of small amplitude but becomes unstable when a disturbance of finite amplitude is provided. This phenomenon where the system is made unstable by providing suitable initial conditions is called triggering in thermoacoustic literature [15]. Triggering was observed in earlier experiments and numerical studies conducted on horizontal Rijke tubes [5–11, 16–18].

Apart from the danger of getting triggered into instability, a subcritical bifurcation is characterized by the abrupt appearance of large amplitude oscillations right at the onset of instability. Furthermore, the value of the system parameter has to be reduced well below the critical value to make the system stable again, due to hysteresis associated with subcritical bifurcation [12–14]. The width of the hysteresis zone, which represents the parameter range where the system is bistable, can be used as an indicator to identify the nature of bifurcation. The presence of hysteresis zone confirms that the transition to instability is subcritical [12–14]. Thus, a study of variation in the width of hysteresis zone becomes significant.

The earlier experiments and numerical studies conducted on horizontal Rijke tubes were aimed at understanding the effect of various system parameters on the stability characteristics of the system. The stability boundaries were experimentally determined for various values of heater power [6, 7]. Numerical studies have provided globally stable, globally unstable and bistable regions for various system parameters such as heater power, heater location, damping coefficient and time lag [9–11]. The nature of transition observed in both experimental and numerical studies was subcritical Hopf bifurcation. Triggering was reported in experiments [6, 7] and in numerical studies [5, 9–11].

Matveev [6] and Mariappan [7] used heater power as the control parameter. Matveev [6] performed experiments in a horizontal Rijke tube and established the stability boundaries for different mass flow rates when heater power was selected as the control parameter. Presence of a hysteresis zone and the phenomenon of triggering were reported by Matveev [6]. Further he found that the width of the hysteresis zone decreased with decrease in mass flow rate. During instability, the system was found to exhibit limit cycle oscillations. Later, Mariappan [7] experimentally determined the triggering

amplitude and reported reduction in the width of the hysteresis zone for a decrease in mass flow rate in a horizontal Rijke tube. The transition to instability was found to be subcritical and limit cycle oscillations were observed.

Balasubramanian & Sujith [5] proposed a model for the horizontal Rijke tube which captured many of the experimentally observed features including the subcritical transition to instability. The bifurcation characteristics of this model for various system parameters such as heater power, heater location, damping coefficients and time lag were studied by Subramanian *et al*. [9] using numerical continuation method and also showed the existence of period doubling route to chaos. Subramanian *et al*. [10] found that the transition to instability happened always through a subcritical Hopf bifurcation for variation in any of the system parameters. Juniper [17] showed that the transition to instability is subcritical when heater power is chosen as the control parameter and found out the most dangerous initial condition using the adjoint optimization technique. In summary, the experimental and numerical investigations conducted on horizontal Rijke tubes indicate that the transition from non-oscillatory to oscillatory state is subcritical in nature [5–11]. Nonetheless experimental studies on horizontal Rijke tube where system parameters other than heater power are varied are not present in the literature to the best knowledge of the authors. The subcritical nature of transition observed in the case of Rijke tube model are not yet confirmed by experimental observations for system parameters such as heater location.

Although some experimental studies allude to the reduction in the width of the hysteresis zone with decrease in mass flow rate [6, 7], further investigations were not performed. It is essential to analyze the influence of system parameters on the presence of bistable region in the context of a horizontal Rijke tube to get a clear idea on the nature of transition. The present work aims to investigate the influence of system parameters on the presence of a bistable region. An attempt is made to understand the nature of criticality of bifurcations by investigating the influence of system parameters such as heater power and heater location on the hysteresis characteristics of the horizontal Rijke tube. The paper is organized as follows. Section 2 describes experimental setup and experimental procedure used for the present study. Section 3 highlights the results obtained. Major conclusions and significant findings are explained in Section 4.

2. EXPERIMENTAL SETUP

The experimental setup consists of a horizontal Rijke tube with a mesh type electric heater. The Rijke tube is 1 m long with a cross-sectional area of 93×93 mm^2. It is made of aluminium plates of 7 mm thickness. The mean flow is established with the help of a blower (1 HP, Continental Airflow Systems, Type CLP-2-1-650) which works in the suction mode. The flow rate is measured with the help of a compact-orifice mass-flow meter (Rosemount 3051 SFC) which is located upstream of the blower. The flow meter can measure a maximum mass flow rate of 5 g/s with an uncertainty of ± 2.1% which results in an uncertainty of ± 3.1% in the measurement of average flow velocity. To eliminate the interaction between the acoustics of the blower and the Rijke tube, a decoupler ($120 \times 45 \times 45$ cm^3) is provided in between, at the outlet end of the Rijke tube. A programmable DC power supply (TDK–Lambda, GEN8–400, 0–8 V, 0–400 A) is used

to power the mesh type heater. The mesh type electrical heater used in the present study is similar to the one used by Matveev [6] and Mariappan [7]. The uncertainty associated with heater power measurement, happens to be 0.4 W which includes the uncertainty in the measurement of voltage and uncertainty in the measurement of current. The advantage of the mesh type heater is that it can provide high amount of electric power (~ 1 kW) for a fairly long duration of time (~ 6 hours) without losing its integrity [6]. A mesh-type heater also ensures uniform heating when compared to a coil type heater. In order to avoid electrical contact with the walls of the tube and also to prevent heat loss to the walls of the tube, a ceramic housing is provided. A traversing mechanism with a least count of 1 mm is used to change the heater location.

The experimental setup used for the present work (Fig. 2) is similar to the one used by Mariappan [7]. A pressure transducer (PCB 103B02) mounted at 30 cm (from the inlet end) is used to measure the acoustic pressure. The sensitivity of the pressure transducer is 217.5 mV/kPa and the uncertainty involved in the pressure measurement is 0.2 Pa. Data is acquired with the help of a National Instruments make PCI 6221 data acquisition card. The data was acquired at a sampling frequency of 10,000 Hz. Thirty thousand data points were acquired in each sample. The bin size used for obtaining the frequency spectra is 0.3 Hz.

In order to ensure uniform ambient conditions, the relative humidity level was maintained in the range of 40% – 50% during all experiments. The initial temperature was maintained at 19 ± 3^0 C. Similarly the experiments were conducted only when the cold decay rate α was $18.5 \pm 5\%$ s^{-1} for the fundamental frequency. The cold decay rate is measured by exciting the system using a loud speaker (Ahuja AU60) mounted at 62.5 cm from the inlet; at the first eigenmode frequency for a short duration of time. Once the loud speaker is switched off, the acoustic pressure decays down. The cold decay rate α is determined by performing the Hilbert transform of the pressure signal and by calculating the logarithmic decay [7].

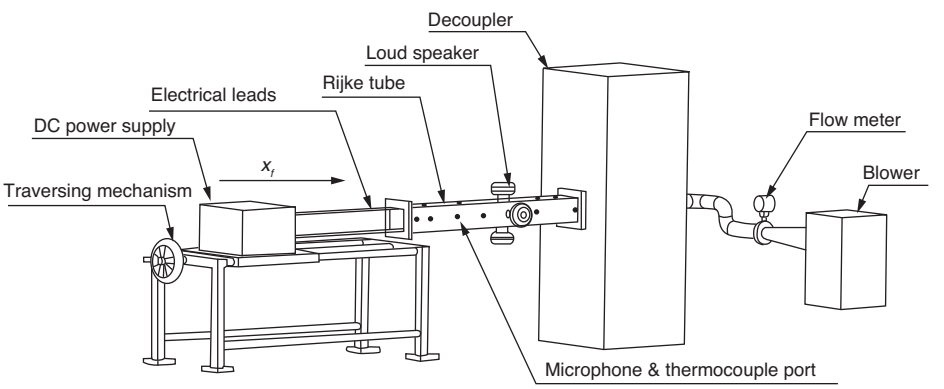

Figure 2: Schematic of the experimental setup. A blower is used to provide the mean flow and a flow meter is used to measure the flow rate. The wire mesh is heated using a D. C. power supply unit. A traversing mechanism is used to change the heater position x_f.

In all the experiments, a bifurcation parameter is varied in fine steps till the system attains its oscillatory state from steady state and then decreasing the bifurcation parameter to bring the system back to steady state. When a particular parameter, say heater power, is chosen as the bifurcation parameter, the other parameters, say heater location, mass flow rate and cold decay rate are maintained constant during a single experiment. Heater power (K) and heater location (x_f) are chosen as the bifurcation parameters in the current set of experiments.

Bifurcation experiments performed by varying the value of heater power are obtained for different mass flow rates (m) namely 1.25 g/s, 1.41 g/s, 1.56 g/s, 1.72 g/s, 1.88 g/s, 2.03 g/s, 2.19 g/s and 2.34 g/s. The heater location is varied continuously for eight different mass flow rates, i.e., for 1.25 g/s, 1.41 g/s, 1.56 g/s, 1.72 g/s, 1.88 g/s, 2.03 g/s, 2.19 g/s, 2.34 g/s and 2.97 g/s. The heater location is measured from the inlet of the duct.

3. RESULTS

3.1. Effect of heater power

We present here the effect of changing the heater power on the system dynamics. We performed experiments by slowly varying the power supplied to the electrical heater. The system was preheated for 20 minutes and the value of acoustic pressure amplitude (P) and the value of heater power (K) were noted down after preheating. The preheating was done in order to lessen the variations in temperature as the heater power is increased [6]. Thereafter, the heater power was increased in a quasi-steady manner. Input voltage to the electrical heater was increased in steps of 0.01 V which corresponds to an increase in electrical power of 2–3 W. If the heater power is increased rapidly, it can cause nonlinear triggering of instability [6]. To avoid this nonlinear triggering of instabilities, a settling time of 2 minutes is imposed between the power increments [6, 7].

During this time, the system achieves a steady state which is confirmed by the steady temperature noted by the thermocouple. Power increment used in the current investigation is 2–3 W, which is comparable to the power increment used by Matveev [6]. However when the heater power was varied in a fine manner, power increment happens to be 0.5 W. Figure 3 shows the bifurcation diagram obtained by varying the heater power (K). The median value of the peak acoustic pressure (P) is plotted against the heater power (K). During the *forward path*, i.e., while K is increased, the system is stable till the point C which corresponds to a heater power of 337 W.

Further increase in heater power takes the system to a stable limit cycle (point D). From D to E, the amplitude of the limit cycle oscillations increases with increase in heater power. Once the system has reached point E, the heater power is decreased in steps of 2-3 W. The asymptotic state achieved by the system during the decrease of heater power is termed as *return path*. The system continues in the state of stable limit cycle oscillations up to point F during the return path. When the heater power is reduced below 308 W, the system reverts back to the non-oscillatory state.

In the forward path, the system is globally stable for low values of K (line AB). Region BC is termed as bistable where the system can be triggered to instability. Beyond the point C, the system is globally unstable. The difference observed between

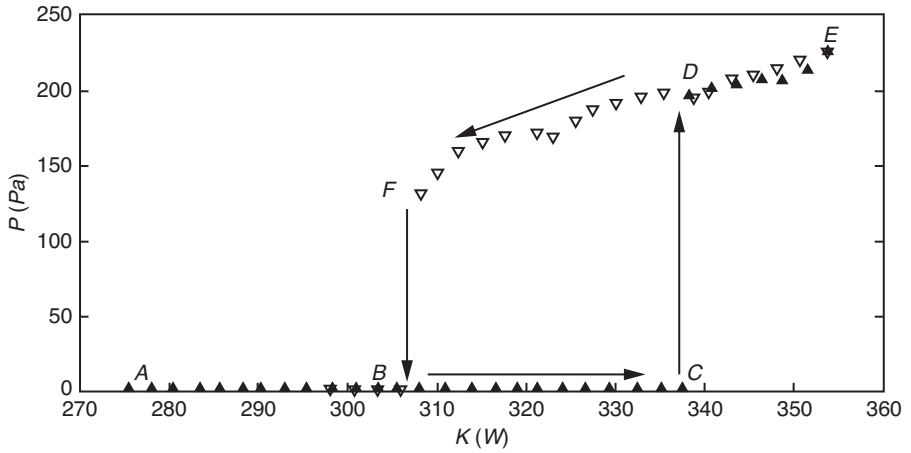

Figure 3: Experimental bifurcation diagram displaying the values of acoustic pressure P measured at x = 30 cm for a quasi-steady variation in the power supplied to heater K. The system undergoes a subcritical Hopf bifurcation at K = 337 W and a fold bifurcation at K = 307 W. *BCDF* represents the hysteresis region where the system is in a bistable state. The heater is located at $x_f = L/4$. Mass flow rate $\dot{m}$ = 2.34 g/s. ▲ - Increasing K, ▽-Decreasing K.

the forward path (*ABCDE*) and the return path (*EDFBA*) establishes the hysteresis zone. Similar results are reported in literature [6, 7].

The asymptotic state of the system can be understood by reconstructing the phase space from the acquired time series. Phase space of a dynamical system is the one which represents all possible states of the system. In general, the phase space will be an *'n'* dimensional vector space constructed using *'n'* state variables. The state variables can be identified from the governing equations of the system. If the governing equations are not known, the phase space can be constructed using indirect methods [19]. One of them happens to be the method of using time-delayed vectors. These time-delayed vectors are constructed using Takens' embedding theorem, from time series data of one of the physical variables [20]. Time delayed vectors are constructed by calculating the optimum time delay. The dimension of the reconstructed phase space will be determined by knowing the embedding dimension. The embedding dimension in the present case is determined by the method of False Nearest Neighbours (FNN). The technique of reconstruction of phase space from experimentally obtained time series data is explained by Kabiraj *et al*. [21] and Nair *et al*. [22] in the context of thermoacoustic instabilities.

The amplitude spectra of the pressure time series signal along with corresponding phase portrait is shown in Figure 3 for a heater power value of 339 W. A prominent frequency of 168.8 Hz can be seen in the amplitude spectra and phase portrait shows a

closed orbit which happens to be a limit cycle (Fig. 4). It is worth mentioning that the prominent frequency 168.8 Hz in the amplitude spectra is nearly equal to the first acoustic mode of a half wave length resonator.

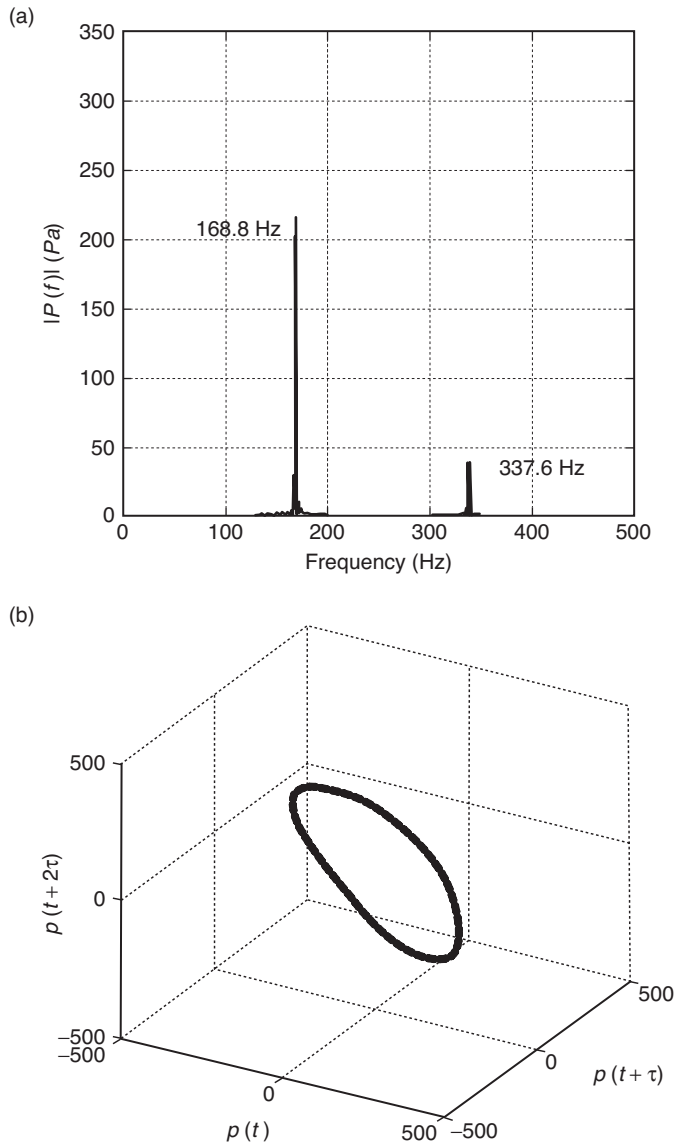

Figure 4: (a) The amplitude spectrum of the pressure time series showing distinct peaks indicating limit cycle oscillations. The bin size used is 0.3 *Hz* (b) Phase portrait reconstructed from pressure time series depicting an isolated closed orbit in the phase space. Heater power K = 339 W. Heater is located at $x_f = L/4$. Mass flow rate $\dot{m}$ = 2.34 g/s.

Presence of the hysteresis zone (Fig. 3) and the limit cycle in the reconstructed phase portrait (Fig. 4b) confirm that the bifurcation is subcritical Hopf bifurcation. In order to understand the effect of mass flow rate on the dynamics of the system, the experiment is performed for different mass flow rates. When the bifurcation plots for low and high mass flow rates are compared, the hysteresis zone is clearly visible in the case of high mass flow rates (Fig. 5c) whereas it becomes unobservable for low mass flow rates (Fig. 5b).

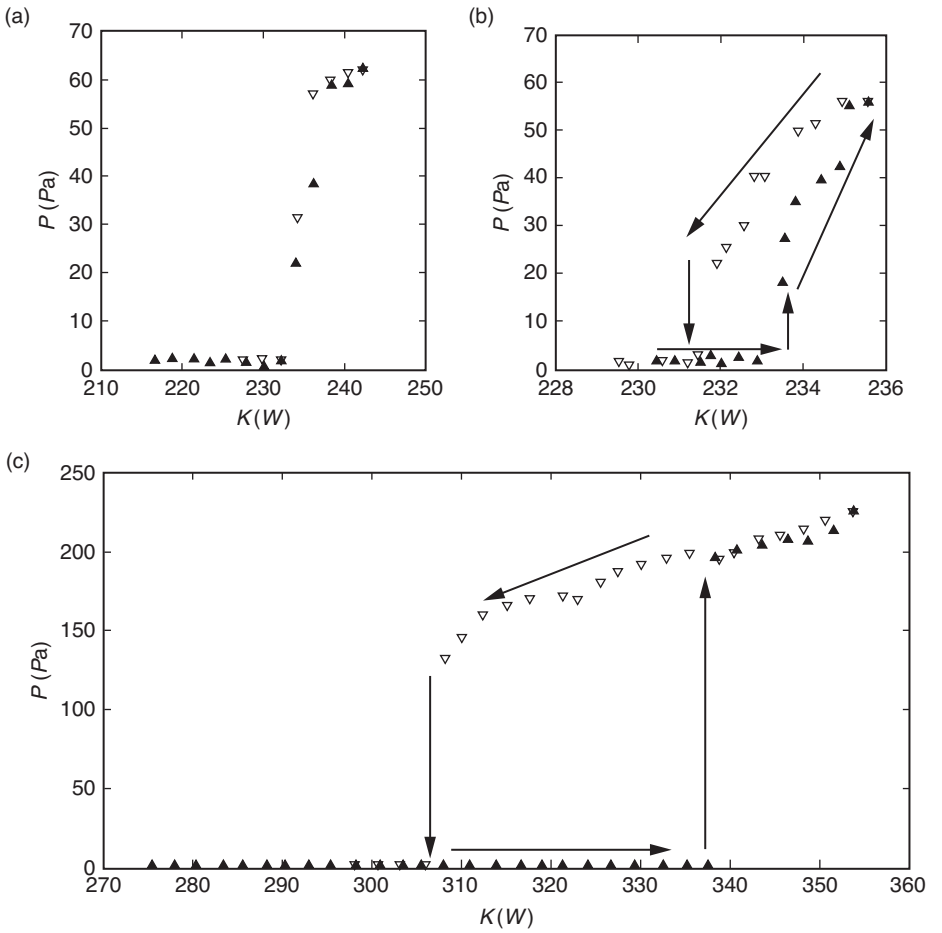

Figure 5: (a) Experimental bifurcation plot for mass flow rate $\dot{m}$ = 1.25 g/s. The heater power is varied with a step size of 2 W. The hysteresis zone is not observable in this case, however there is a sudden jump in the value of acoustic pressure during the transition (b) Experimental bifurcation plot for mass flow rate $\dot{m}$ =1.25 g/s. The heater power is varied with step size of 0.5 W. The hysteresis zone is observable with this fine variation in the control parameter. (c) Experimental bifurcation plot for mass flow rate $\dot{m}$ = 2.34 g/s. The heater power is varied with a step size of 2 W. The hysteresis is clearly observable. The heater is located at $x_f = L/4$. ▲-Increasing K, ▽-Decreasing K.

For low mass flow rates, the forward and reverse paths appear to merge together (Fig. 5a) and the hysteresis zone is not observable as in the case of high mass flow rates (Fig. 5c). Even though the hysteresis zone is not observable, a discrete jump in acoustic pressure can be seen during the transition for low mass flow rate (Fig. 5a). The sudden jump observed in the acoustic pressure confirms that the transition is subcritical even for low mass flow rates [12]. Since subcritical transitions are characterized by the presence of a hysteresis zone, we performed the experiments with fine variation in control parameter, to detect the hysteresis zone present near the transition point. The heater power is varied in a quasi-steady manner with a step size of 0.5 W. The bifurcation diagram with fine variation in heater power is depicted in Fig. 5b. It can be seen that in the case of finer variation in control parameter the hysteresis zone is clearly observable.

Similar set of experiments were performed for mass flow rates 1.41 g/s, 1.56 g/s and 1.72 g/s. For all these four mass flow rates, i.e., for 1.25 g/s, 1.41 g/s, 1.56 g/s and 1.72 g/s the hysteresis zone is not detectable when the heater power is varied in a coarse manner with a step size of 2 W. However there exists a definite jump in the value of acoustic pressure near the transition. When the step size is reduced to 0.5W the hysteresis zone became clearly observable for all the four mass flow rates.

3.2. Effect of heater location

We now discuss the effect of heater location on the hysteresis characteristics of a horizontal Rijke tube. Experiments were conducted by varying the heater location in a quasi-steady manner. The system was preheated for 20 minutes to reduce the variation in temperature along the duct. The heater was located at the inlet end before the start of the experiment. The value of the acoustic pressure amplitude (P) and the value of heater location (x_f) were recorded after preheating. Heater location was changed in steps of 1 cm and a settling time of one minute is chosen. The heater location is measured from the inlet. When the heater is located at the inlet end, x_f is considered as zero. The variation in the median value of the peak acoustic pressure with variation in heater location is shown in Fig. 6.

During the forward path, when x_f is increased, the system is stable until x_f becomes 19 cm. The system undergoes a Hopf bifurcation at x_f = 19 cm. Thereafter, the amplitude of pressure oscillations increases and reaches a maximum at x_f = 33 cm.

Further increase in x_f causes a decrease in the pressure amplitude and the system goes back abruptly to the steady state when x_f = 36 cm. While in the reverse path, when x_f is decreased, the system remains stable till x_f = 29 cm. When the heater is located at 29 cm away from the inlet, the system undergoes a Hopf bifurcation and reaches a state of stable limit cycle oscillations. As the heater is moved towards the inlet, x_f is decreased; the amplitude of oscillations decreases and the system reverts to the steady state when the heater is located at 18 cm away from the inlet. A clear hysteresis zone is present near the second Hopf point (29 cm). Although the hysteresis zone is not observable near the first Hopf point (19 cm) for coarse variation in heater location, a definite jump in the value of acoustic pressure near the transition point can be observed. However with fine variation in heater location, the hysteresis zone near the first Hopf point also becomes detectable as shown in the inset of Fig. 6.

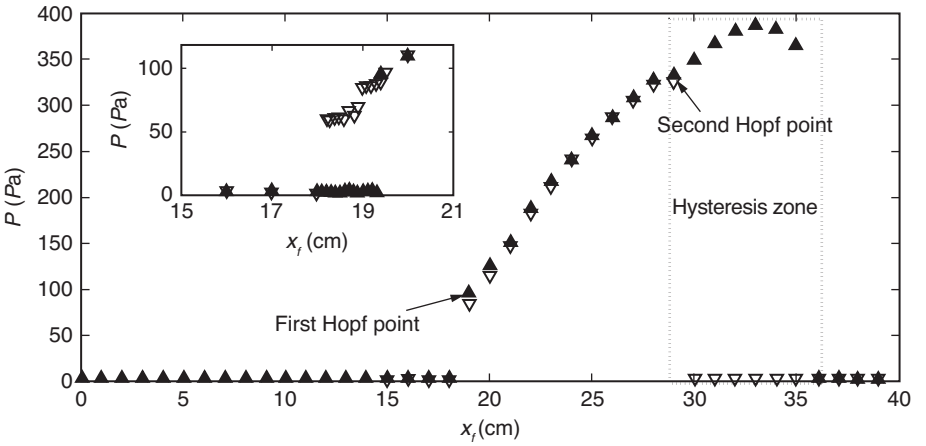

Figure 6: Experimental bifurcation diagram displaying the values of acoustic pressure at x = 30 cm for a quasi-steady variation in the heater location x_f. Subcritical Hopf bifurcation happens at x_f = 19 cm during the forward path and at x_f = 29 cm during the reverse path. Hysteresis zone near the second Hopf point is observable with coarse variation in heater location and the hysteresis zone near the first Hopf point is shown only with fine variation in heater location (see inset). The heater power K = 423 W. Mass flow rate $\dot{m}$ = 2.34 g/s. ▲- Increasing x_f , ▽ - Decreasing x_f.

Figure 7 shows the Fourier transform of the pressure signal and phase portrait of the system when the heater is located at 19 cm; i.e. at first Hopf point. The FFT shows a prominent frequency of 169 Hz and the phase portrait is a limit cycle. Just as in the case of heater power, here also the prominent frequency corresponds to the first acoustic mode of a duct with open-open boundary condition. From the presence of a prominent frequency in FFT and the appearance of limit cycle in the phase portrait, it can be concluded that the bifurcation occurring at x_f = 19 cm is Hopf bifurcation.

During the return path, the FFT shows a prominent frequency and the phase portrait is a limit cycle when the heater is located at 29 cm (Fig. 8). The presence of a prominent frequency along with the presence of a limit cycle indicates that the system undergoes Hopf bifurcation during the return path. The presence of the hysteresis zone along with the presence of discrete jump in the value of acoustic pressure near the transition point indicates that the transition is subcritical for both first and second Hopf points (19 cm and 29 cm). The presence of two Hopf points and the subcritical nature of transition observed at both of them is consistent with the results reported by Subramanian *et al* . [9].

The experiments where heater location is continuously changed for a fixed heater power were performed for different values of mass flow rate. A comparison between the bifurcation diagrams obtained for 1.25 g/s (Fig. 9a) and for 2.34 g/s (Fig. 9b) is shown in Fig. 9.

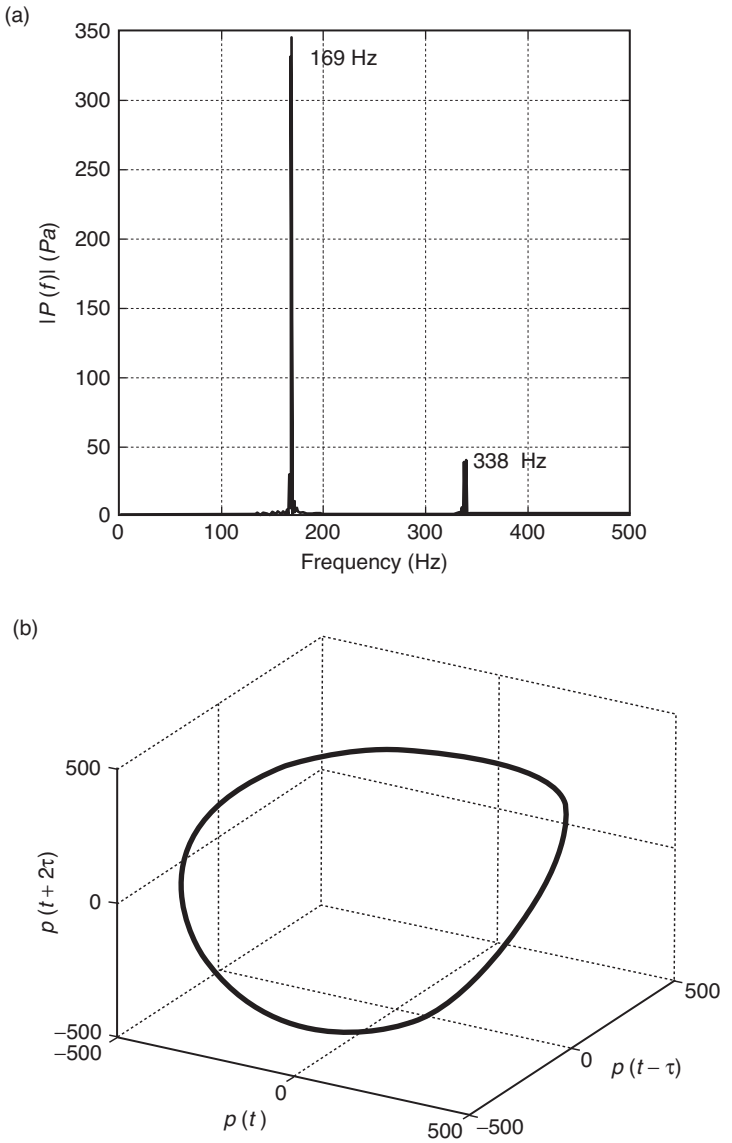

Figure 7: (a) The amplitude spectrum of the pressure time series showing distinct peaks indicating limit cycle oscillations. The bin size used is 0.3 Hz (b) Phase portrait reconstructed from pressure time series depicting an isolated closed orbit in the phase space. Heater is located at x_f = 19 cm. Heater power K = 423 W. Mass flow rate $\dot{m}$ = 2.34 g/s.

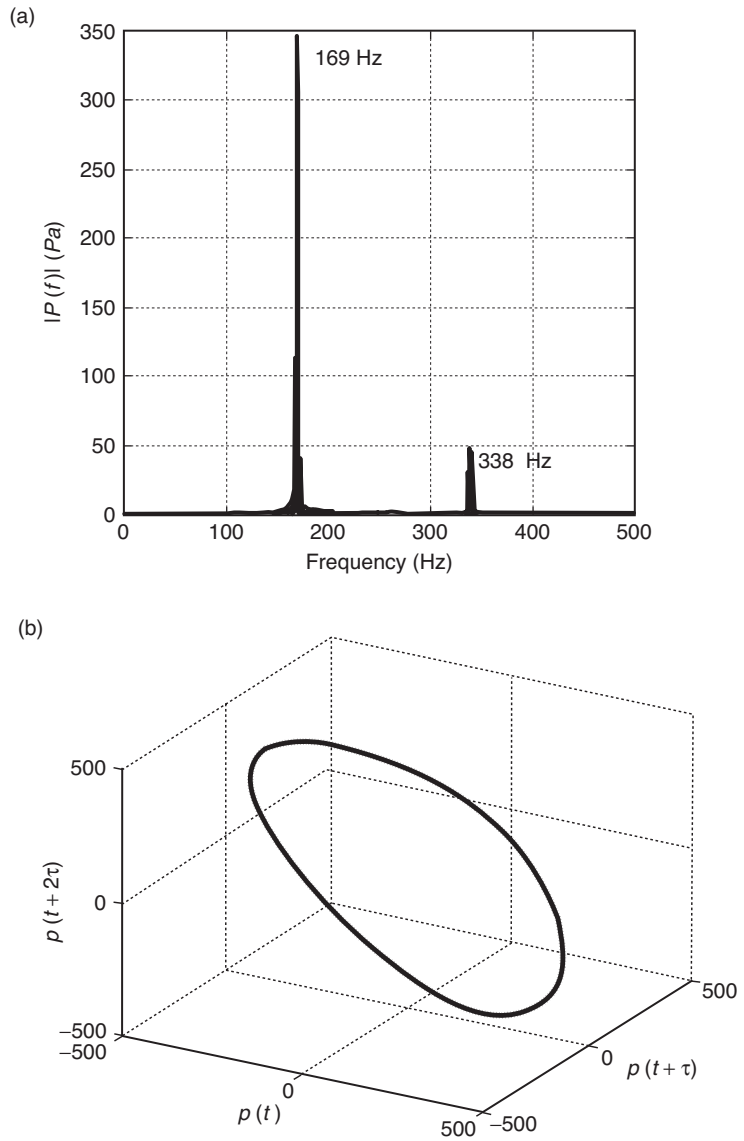

Figure 8: (a) The amplitude spectrum of the pressure time series showing distinct peaks indicating limit cycle oscillations. The bin size used is 0.3 Hz (b) Phase portrait reconstructed from pressure time series depicting an isolated closed orbit in the phase space. Heater is located at x_f = 29 cm. Heater power K = 423 W. Mass flow rate $\dot{m}$ = 2.34 g/s.

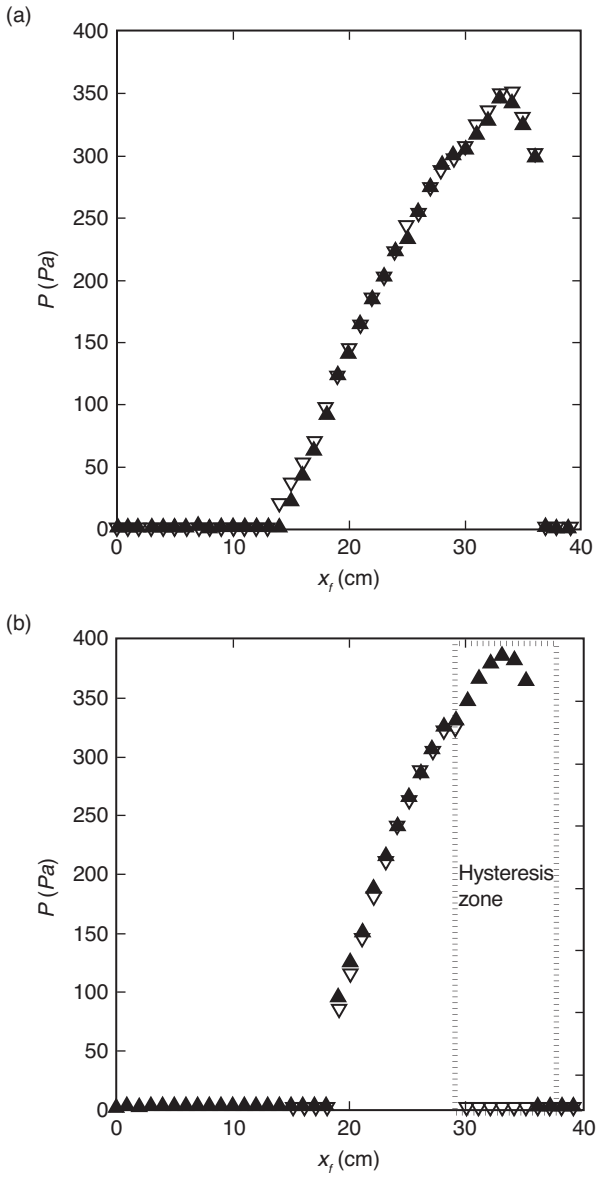

Figure 9: Experimental bifurcation diagrams displaying the variation of acoustic pressure P at x = 30 cm with a quasi-steady variation of heater location x_f (a) for mass flow rate $\dot{m}$ = 1.25 g/s and (b) for mass flow rate $\dot{m}$ = 2.34 g/s. The hysteresis zone is not observable for $\dot{m}$ = 1.25 g/s whereas the hysteresis zone is observable for $\dot{m}$ = 2.34 g/s. The heater power K = 423 W. ▲- Increasing x_f; ▽-Decreasing x_f.

When the mass flow rate is decreased, the hysteresis zone near the second Hopf point becomes undetectable and the forward and reverse paths appear to merge together. Even when the hysteresis zone becomes undetectable, a definite jump in the amplitude of acoustic pressure is seen during transition and the observed jump is sufficiently above the noise floor. This jump observed in the amplitude of acoustic pressure confirms that the transition is subcritical [12]. The variation in the control parameter, heater location, is made finer to detect the hysteresis zone as in the case of heater power. As the heater location is varied in a finer manner, with a step size of 1 mm, near the Hopf point, the hysteresis zone becomes observable for the case of 1.25 g/s.

The bifurcation diagrams with fine variation in control parameter are shown in Fig. 10. It is observed that the hysteresis zone is detectable for a fine variation of the control parameter. Since the width of the hysteresis zone is much smaller than the overall range in which the control parameter is varied, only the portion of the hysteresis zone near the Hopf point is shown in Fig. 10. Even for a low mass flow rate of 1.25 g/s, we can conclude that the transition to instability is clearly subcritical when the heater location is chosen as the control parameter. The subcritical nature of the transition to instability is confirmed by the presence of hysteresis zone and a discrete jump in the values of acoustic pressure during transition (Fig. 10 a & b) [12].

The experiment is performed for different mass flow rates by varying the heater location in a fine manner. We find that a hysteresis zone of definite width exists even for very low mass flow rates. However, for the case of low mass flow rates, the hysteresis zone is often perceptible only when the parameter variation is made finer.

The experiment was performed for a mass flow rate of 2.97 g/s to understand the system dynamics at a higher mass flow rate. The power supplied to the heater in the earlier experiments was found to be insufficient to make the system unstable at a mass flow rate of 2.97 g/s. So the heater power is increased from its previous value of 423 W to 482 W. Since the heater power was changed, the results for the mass flow rate of 2.97 g/s are presented separately. It can be observed that there are two distinct regimes of heater location for which oscillations are present (Regions 1&2 in Fig. 11). The absence of oscillations near the open end is due to the fact that the acoustic pressure becomes zero at the open end. Since the acoustic velocity becomes zero at $L/2$, thermoacoustic instability does not occur as the heater is moved near this point. For the heater power value (482 W) used in the present study, instability did not occur when the heater was located beyond $L/2$.

When the heater is located at 8 cm from the inlet, the system undergoes a subcritical Hopf bifurcation. The subcritical nature of transition can be confirmed by the discrete jump in the value of acoustic pressure when x_f is 8 cm (Region 1 in Fig. 11). Figure 11 shows the Fourier transform of pressure time series and the corresponding reconstructed phase portrait when the heater is located at 8 cm away from the inlet. The presence of a distinct frequency of 352.8 Hz which is approximately equal to the frequency of the second acoustic mode of a half wavelength resonator (Fig. 12a) and the presence of a limit cycle in the reconstructed phase portrait (Fig. 12b) confirm that the system undergoes a subcritical Hopf bifurcation.

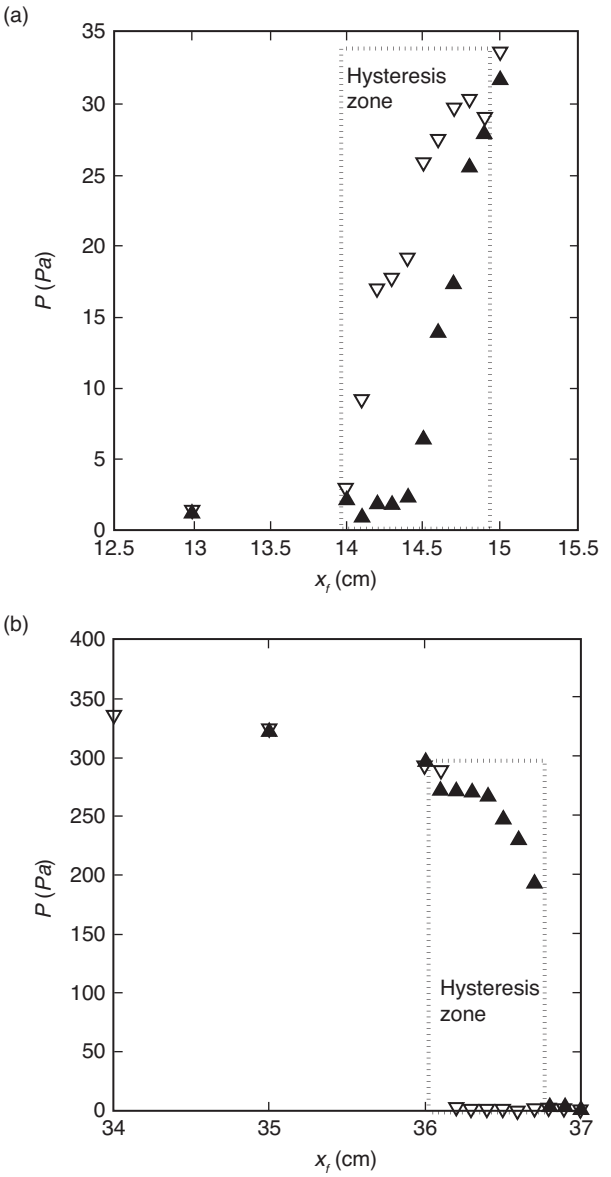

Figure 10: Experimental bifurcation diagram displaying the values of acoustic pressure at $x = 30$ cm versus the location of the heater (a) near the first Hopf point and (b) near the second Hopf point. Heater location is varied in fine steps of 1 mm. With this fine variation in heater location, the hysteresis zones at first and second Hopf points become observable. The heater power $K = 423$ W. Mass flow rate $\dot{m} = 1.25$ g/s. ▲- Increasing x_f; ▽- Decreasing x_f.

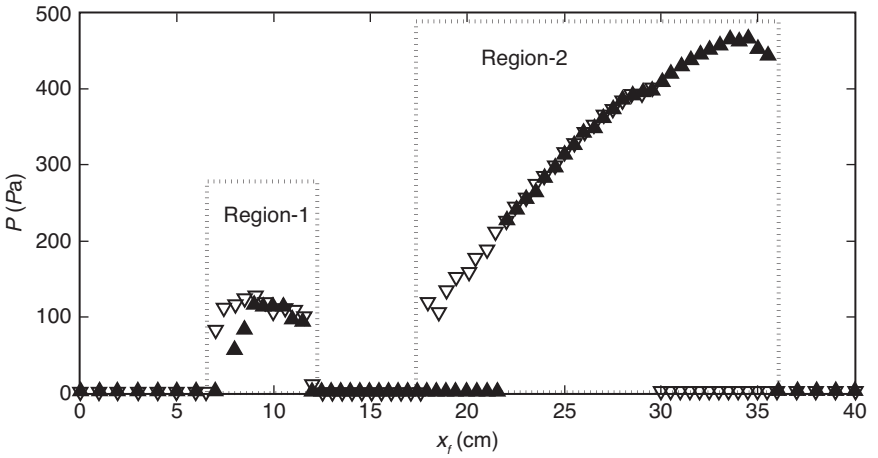

Figure 11: Experimental bifurcation diagram displaying the variation of acoustic pressure P at x = 30 cm for a quasi steady variation in the heater location x_f for a mass flow rate of $\dot{m}$ = 2.97 g/s. Two distinct regions of instability can be seen. The bifurcations that happen in both region-1 and region-2 are subcritical Hopf bifurcations confirmed by the presence of hysteresis zones. The heater power K = 482 W. ▲-Increasing x_f ; ▽- Decreasing x_f.

Figure 13 depicts the local maxima of the pressure time series with heater location, for forward path (Fig. 13a) and for reverse path (Fig. 13b). It can be observed that the local maxima has a single value till x_f = 9 cm during the forward path and till x_f = 8.5 cm during the reverse path. After that two branches are born. The presence of two distinct branches is a characteristic feature of period-2 oscillations [12]. These two branches represent the two distinct values of local maxima of pressure time series. Before the onset of period-2 oscillations, the acoustic pressure has single local maxima. Once the period-2 oscillations set in, the local maxima of pressure time series has 2 distinct values. It should be observed that till x_f = 9 cm in the forward path and till x_f = 8.5 cm during the reverse path, the second mode alone is linearly unstable in Region-1. Whereas after the heater locations 9 cm and 8.5 cm in the forward and reverse paths respectively, first mode also becomes linearly unstable which gives rise to the occurrence of period-2 oscillations.

The presence of period-2 orbit can be clearly seen in Figure 14. A new frequency of the oscillations of value 176.4 Hz which is quite close to the frequency of first acoustic mode gets introduced as the heater is moved from 9.5 cm to 10 cm (Fig. 14a). The value of the new frequency happens to be exactly half of the existing one. This marks the onset of period-2 oscillations. The phase portrait pertinent to the aforementioned heater location represents a double loop (Fig. 14b).

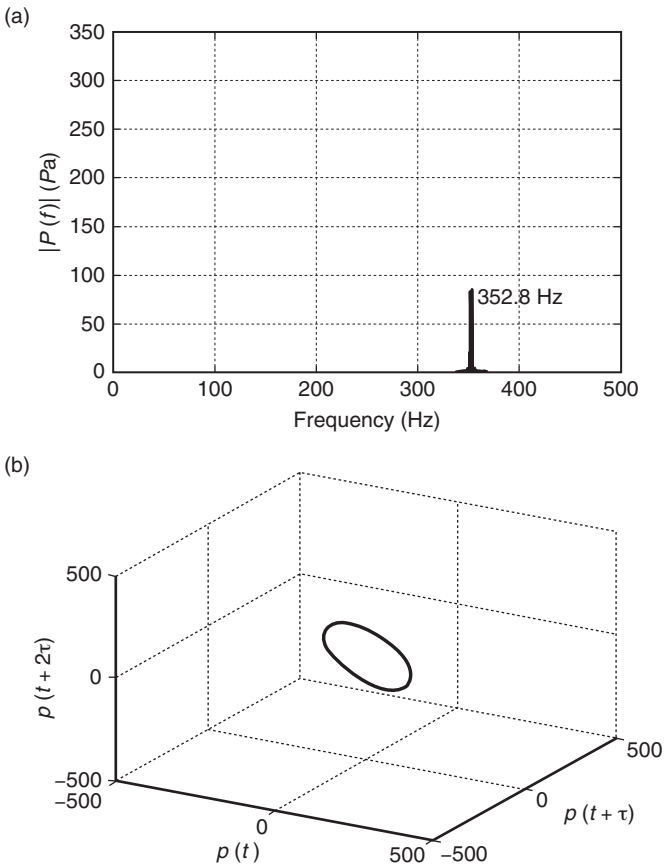

Figure 12: (a) The amplitude spectrum of the pressure time series showing distinct peak indicating limit cycle oscillations. The bin size used is 0.3 Hz (b) Phase portrait reconstructed from pressure time series depicting an isolated closed orbit in the phase space. Heater is located at x_f = 8 cm. Heater power K = 482 W. Mass flow rate $\dot{m}$ = 2.97 g/s.

The presence of a period-2 orbit is in agreement with the observations made by Subramanian *et al*. [9]; they reported the presence of a period-2 orbit for a non-dimensional heater location of 0.1. The length of the Rijke tube used in the present study is 1 m, thus the non-dimensional heater location at which period-2 orbit is found happens to be 0.095. This is quite close with the value reported by Subramanian *et al* [9].

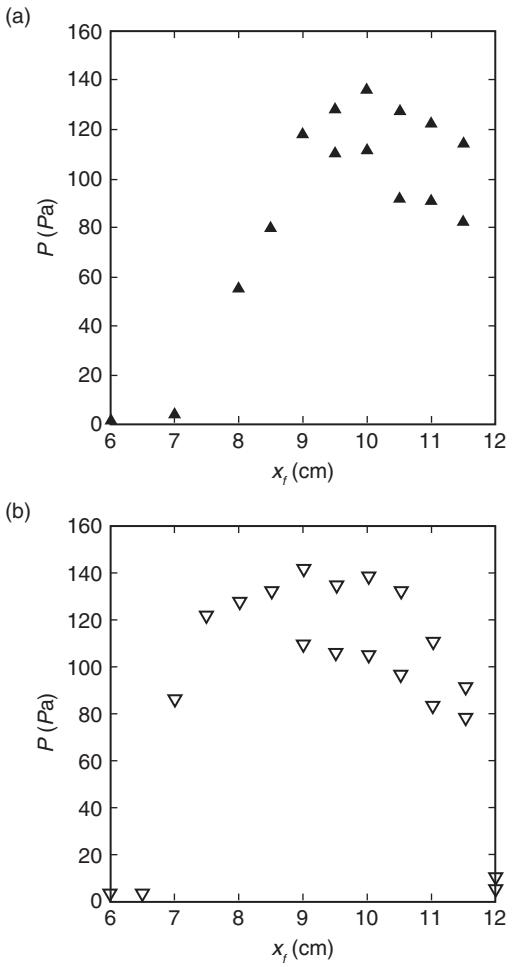

Figure 13: Variation of peak pressure P at x = 30 cm for a quasi steady variation of the heater location x_f (a) during the forward path (b) during the return path showing the presence of period-2 oscillations for a mass flow rate $\dot{m}$ = 2.97 g/s. K = 482 W. ▲-Increasing x_f. ▽- Decreasing x_f.

3.3. Variation of hysteresis width with mass flow rate

In this section, we discuss the variation in the hysteresis width with mass flow rate when any of the control parameter, say heater power or heater location, is changed continuously while the other parameter is maintained constant. The variation of non-dimensional hysteresis width with Strouhal number is shown in Fig. 15. Non-dimensional hysteresis width and Strouhal number are calculated as

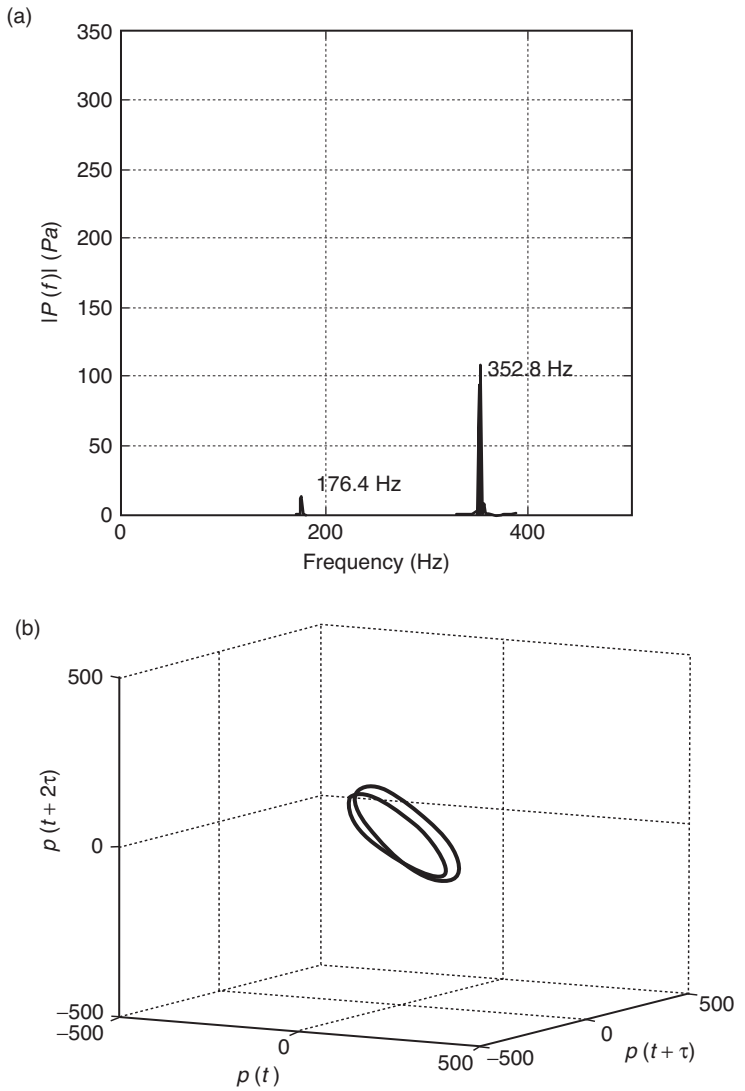

Figure 14: (a) The amplitude spectrum of the pressure time series showing distinct peaks at f and $f/2$, where f is 352.8 Hz, indicating period-2 oscillations. The bin size used is 0.3 Hz (b) Phase portrait reconstructed from pressure time series depicting a double loop in the phase space. Heater is located at x_f = 10 cm. Heater power K = 482W. Mass flow rate $\dot{m}$ = 2.97 g/s.

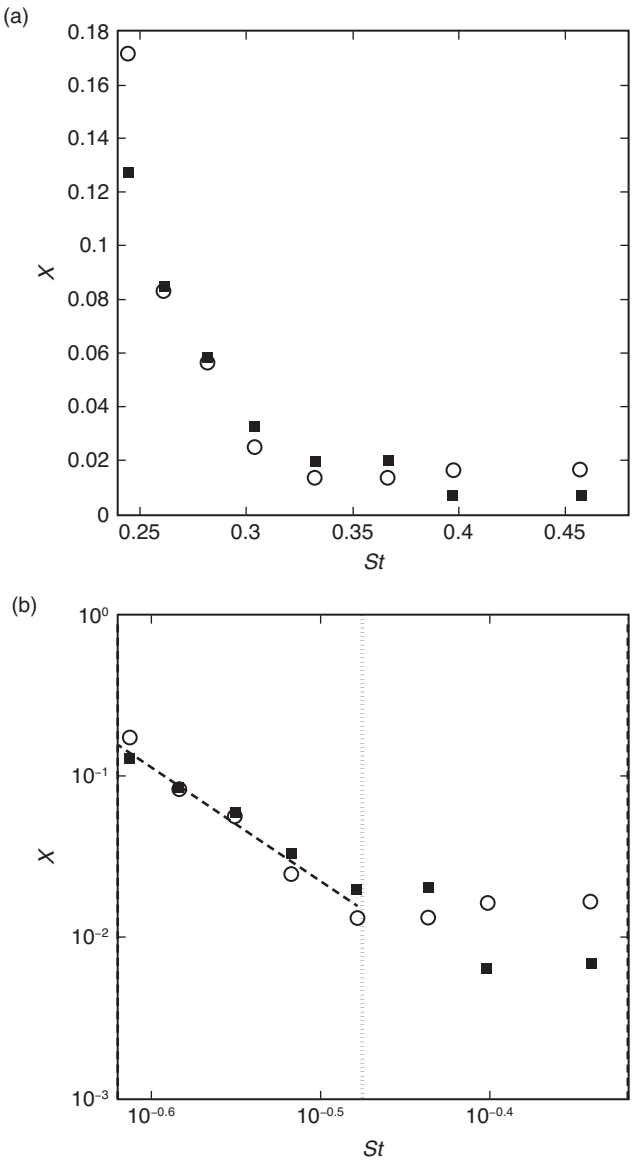

Figure 15: Variation of non-dimensional hysteresis width χ with Strouhal number St shown in (a) Linear scale and in (b) Log-Log scale. It can be seen that the non-dimensional hysteresis widths are same for heater power and heater location for a range of Strouhal numbers and there exists a power law relation. ■-Heater power, ○ -Heater location.

Non-dimensional hysteresis width = $\chi = \{|\mu_H - \mu_f| / \mu_H\}$ (1)

Strouhal number = St = {Flow time scale/Acoustic time scale} (2)

Flow time scale = $\{d_w \rho A / \dot{m}\}$ (3)

Acoustic time scale = $\{2L / c_0\}$ (4)

Where,

μ_H = Parameter value at the Hopf point

μ_f = Parameter value at the fold point

c_0 = Speed of sound at ambient temperature

d_w = Diameter of the heater wire

ρ = Mean density

A = Area of the duct

L = Length of the duct

It is interesting to note that the variation of the non-dimensional hysteresis width as a function of Strouhal number is nearly identical for both heater power and heater location. The width of the hysteresis zone decreases with increase in Strouhal number for both heater power and for heater location. Nevertheless, even for high values of Strouhal number, there exists a definite hysteresis zone which indicates that the transition to instability is subcritical in nature (Fig.15a) for the range of parameters covered in this study. The uncertainty in non-dimensional hysteresis width for heater power and heater location happens to be 0.003 and 0.004 respectively. The minimum non-dimensional hysteresis width reported is 0.006 in the case of heater power and 0.016 in the case of heater location; these minimum values are well above the uncertainties involved in the measurements. Figure 15b shows the variation of non-dimensional hysteresis width with Strouhal number in a log-log scale. It can be seen that there is a linear relation between non-dimensional hysteresis width and Strouhal number up to a Strouhal number value of 0.33. This is suggestive of a power law dependence of hysteresis width on Strouhal number in the range of Strouhal numbers from 0.24 to 0.33. A vertical dashed line marks the end of the Strouhal number regime where power law dependence of hysteresis width is present.

4. CONCLUSIONS

The heater power and the heater location were varied systematically, one at a time, in the present study. It is found that the width of the hysteresis zone decreases as the mass flow rate is decreased. The presence of the hysteresis zone along with a finite jump in the acoustic pressure near the transition point indicates that, irrespective of the value of mass flow rate, the transition is subcritical in all the experiments we performed. For low mass flow rates, although the hysteresis zone was observed only when the control parameter was varied in a fine manner a finite jump in acoustic pressure near the transition point is always present. Therefore, it is extremely important to ensure that the variation in the parameter is fine enough before a bifurcation can be attributed as

supercritical. Moreover a power law relation is established between non-dimensional hysteresis width and Strouhal number.

It is also found that the non-dimensional hysteresis widths in the case of heater power and heater location are the same for a range of Strouhal numbers. This equivalence suggests a universal bifurcation behaviour which needs to be investigated in detail. When heater location was chosen as the control parameter, period-2 oscillations were observed for some specific values of heater power and mass flow rate. The presence of period-2 oscillations is suggestive of a period doubling route to chaos, however detailed experimental studies need to be performed in order to ensure the same. In summary, this work emphasises the need to thoroughly investigate the presence of hysteresis region before pronouncing a bifurcation as supercritical.

ACKNOWLEDGEMENTS

The authors would like to acknowledge ONR Global for the financial support (Contract Monitors: Dr. Gabriel Roy & Dr. Ramesh Kolar). The authors gratefully acknowledge Mr. Vineeth Nair (IIT Madras) for the valuable discussions that he had with us on the reason for the existence of hysteresis zone and for providing the MATLAB code for phase space reconstruction. Authors would like to thank Dr. Priya Subramanian (Max Planck Institute, Göttingen) for valuable suggestions, critical comments and Dr. Sathesh Mariappan (IIT Kanpur) for the help provided in setting up the experimental setup. Authors would also like to express their gratitude to Mr. Dhileesh (IIT Madras) for the help provided in preparing the schematic of the experimental setup.

REFERENCES

[1] K. R. McManus, T. Poinsot, and S. M. Candel. A review of active control of combustion instabilities. *Progress in Energy and Combustion Science*, 1993, 19, 1–29.

[2] J. W. S. Rayleigh. The explanation of certain acoustical phenomena. *Nature*, 1878, 18, 319–321.

[3] J. Kopitz and W. Polifke. CFD-based application of the Nyquist criterion to thermo-acoustic instabilities. *Journal of Computational Physics*, 2008, 227, 6754–6778.

[4] M. A. Heckl. Nonlinear acoustic effects in the Rijke tube. *Acustica*, 1990, 72, 63–71.

[5] K. Balasubramanian and R. I. Sujith. Thermoacoustic instability in a Rijke tube: Non-normality and nonlinearity. *Physics of Fluids*, 2008, 20, 044103.

[6] K. I. Matveev. Thermo-acoustic instabilities in the Rijke tube: Experiments and modeling. Ph. D. thesis, 2003 California Institute of Technology, Pasadena.

[7] S. Mariappan. Theoretical and experimental investigation of the non-normal nature of thermoacoustic interactions. Ph. D. thesis, 2011, Indian Institute of Technology Madras.

[8] S. Mariappan and R. I. Sujith. Modelling of nonlinear thermoacoustic instability in an electrically heated Rijke tube. *Journal of Fluid Mechanics*, 2011, 680, 511–533.

[9] P. Subramanian, S. Mariappan, R. I. Sujith, and P. Wahi. Bifurcation analysis of thermoacoustic instability in a horizontal Rijke tube. *International Journal of Spray and Combustion Dynamics*, 2010, 2, 325–355.

[10] P. Subramanian, R. I. Sujith, and P. Wahi. Subcritical bifurcation and bistability in thermoacoustic systems. *Journal of Fluid Mechanics*, 2013, 715, 210–238.

[11] P. Subramanian. Dynamical systems approach to the investigation of thermoacoustic instabilities. Ph. D. thesis, 2011, Indian Institute of Technology Madras.

[12] S. H. Strogatz. Nonlinear Dynamics and Chaos: with applications to Physics, Biology, Chemistry, and Engineering, 2000, Westview Press, Colorado.

[13] D. M. James. Differential Dynamical Systems, 2007, Society for Industrial Applied Mathematics, Philadelphia.

[14] R. C. Hilborn. Chaos and nonlinear dynamics: an introduction for scientists and engineers, 2000, Oxford University Press, second edition.

[15] J. M. Wicker, W. D. Greene, S. I. Kim, and V. Yang. Triggering of longitudinal combustion instabilities in rocket motors-nonlinear combustion response. *Journal of Propulsion and Power*, 1996, 12, 1148–1158.

[16] N. Ananthakrishnan, S. Deo, and F. E. C. Culick. Reduced-order modeling and dynamics of nonlinear acoustic waves in a combustion chamber. *Combustion Science and Technology*, 2005, 177, 221–248.

[17] M. P. Juniper. Triggering in the horizontal Rijke tube: non-normality, transient growth and bypass transition. *Journal of Fluid Mechanics*, 2011, 667, 272–308.

[18] I. C. Waugh and M. P. Juniper. Triggering in a thermoacoustic system with stochastic noise. *International Journal of Spray and Combustion Dynamics*, 2011, 3, 225–242.

[19] H. D. I. Abarbanel and J. P. Gollub. The analysis of observed chaotic data in physical systems. *Review of Modern Physics*, 1996, 65, 1331–1392.

[20] F. Takens. Detecting strange attractors in turbulence. *in D. Rand and L. S. Young*, editors, Dynamical Systems and Turbulence, 1980, 898, 366–381.

[21] L. Kabiraj and R. I. Sujith. Nonlinear self-excited thermoacoustic oscillations: intermittency and flame blowout. *Journal of Fluid Mechanics*, 2012, 713, 376–397.

[22] V. Nair, G. Thampi, S. Karuppusamy, S. Gopalan and R. I. Sujith. Loss of chaos in combustion noise as a precursor of impending combustion instability. *International Journal of Spray and Combustion Dynamics*, 2013, 5, 273–290.